

Imprecise probability analysis of steel structures subject to atmospheric corrosion

Hao Zhang^{a,*}, Loc Ha^{a,1}, Quanwang Li^{b,2}, Michael Beer^{c,3}

^a*School of Civil Engineering, The University of Sydney, NSW 2006, Australia*

^b*Department of Civil Engineering, Tsinghua University, Beijing 100084, China.*

^c*Institute for Computer Science in Civil Engineering, Leibniz University Hannover, Germany. Institute for Risk and Uncertainty, University of Liverpool, Liverpool, UK. International joint Research Center for Engineering Reliability and Stochastic Mechanics (ERSM), Tongji University, Shanghai, China.*

Abstract

Evaluating the behaviour of deteriorating steel structures is complicated by the inherent uncertainties in the corrosion process. Theoretically, these uncertainties can be modeled using a probabilistic approach. However, there are practical difficulties in identifying the probabilistic model for the deterioration process as the actual corrosion data are rather limited. Also, the dependencies between different random variables are often vaguely known and, thus, not included in the modeling. This paper proposes a probabilistic analysis framework for modeling the atmospheric corrosion of steel structures with incomplete information. The framework is based on the theory of imprecise probability and copula. Two examples are presented to illustrate the methodology. The role of epistemic uncertainties on structural reliability is investigated through the examples.

Keywords: atmospheric corrosion, corrosion, copula, deterioration,

*Corresponding author (H. Zhang). Tel.: +61293513923, E-mail address: hao.zhang@sydney.edu.au

¹E-mail address: loc.ha@sydney.edu.au

²E-mail address: li_quanwang@tsinghua.edu.cn

³E-mail address: beer@bauinf.uni-hannover.de

1 **1. Introduction**

2 For the safety assessment of deteriorating steel structures, it is crucial to
3 develop a reliable probabilistic model of deterioration to predict the temporal
4 changes to structural resistance [1, 2]. The deterioration of steel structures is
5 a stochastic process with high uncertainties and variabilities. Recent works
6 have treated the uncertainties using a pure probabilistic approach [3, 4]. This
7 approach requires that all statistical characteristics for each uncertainty can
8 be determined reliably from sufficient observational data. In practice, how-
9 ever, available real-world data on structural corrosion are very limited, and
10 the selection of probabilistic models (e.g., distribution type and/or distri-
11 bution parameters) for uncertain variables is so generally based on limited
12 information and/or subjective judgment.

13 It is thus advisable to consider the distribution itself as uncertain when
14 the available data is limited. Statistical estimations provide us with distri-
15 bution functions for the sampling uncertainty, which depends on the sample
16 size. This uncertainty is reducible with an increasing amount of informa-
17 tion/data. From this angle, it may be understood as epistemic uncertainty.
18 Within a pure probabilistic framework, epistemic uncertainty can be handled
19 with Bayesian approaches. Uncertain parameters of a probabilistic model can
20 be described with prior distributions and updated by means of even limited
21 data. They can then be modeled by Bayesian random variables and intro-
22 duced formally, together with the remaining (aleatory) uncertainties, in the
23 probabilistic analysis [5]. Judgmental information is needed to characterize
24 the epistemic uncertainties. The characterization of the epistemic uncertain-
25 ties can be substantiated by using the Bayesian updating rule when data

26 become available. However, when the data is very limited, the result of the
27 Bayesian approach remains as almost purely subjective.

28 Alternatively, an imprecisely known probability distribution can be mod-
29 eled by a family of all candidate probability distributions which are compati-
30 ble with available data. This is the idea of the theory of imprecise probabili-
31 ties [6]. Dealing with a set of probability distributions is essentially different
32 from a Bayesian approach. A practical way to represent the distribution
33 family is to use a probability bounding approach by specifying the lower and
34 upper bounds of the imprecise probability distribution. This corresponds
35 to the use of an interval to represent an unknown but bounded number.
36 Consequently, a unique failure probability cannot be determined. Instead,
37 the failure probability is obtained as an interval whose width reflects the
38 imprecision of the distribution model in the calculated reliability.

39 A popular uncertainty model using the probability bounding approach is
40 the probability box (p-box for short) structure [7]. A p-box is closely related
41 to other set-based uncertainty models such as random sets, fuzzy probabili-
42 ties, Dempster-Shafer evidence theory and random intervals. In many cases,
43 these uncertainty models can be converted into each other, and thus consid-
44 ered to be equivalent [7–10]. Therefore, the p-box approach presented in this
45 paper is also applicable to other set-based uncertainty models. The approach
46 of imprecise probability generally requires less subjective information than
47 the Bayesian approach. It can be argued that, from a frequentist point of
48 view, the epistemic uncertainties in the probability distribution can be more
49 faithfully represented using a probability bounding approach [6, 7, 11].

50 Conventional probabilistic analysis often neglects the correlations and de-
51 pendencies between random variables. This assumption is a common practice
52 partly due to its mathematical convenience, but more likely due to the limited

53 availability of data. It has been shown that the wrong assumption of depen-
54 dence can lead to unreliable predictions for risk assessments [12]. Copula
55 theory is a powerful tool for the dependence modeling of multivariate data.
56 A copula is a joint cumulative distribution function (CDF) with uniform
57 marginal. Copula theory has been used to model dependence in probabil-
58 ity boxes. Ref. [12] proposed a dependence bounds convolution approach
59 in which the uncertainties are modelled as Dempster-Shafer structures and
60 the dependence is expressed as a given parametric copula. This method is
61 useful for calculations of basic arithmetic operations with small numbers of
62 variables. In [13], copula theory is combined with random sets for computing
63 the lower and upper bounds of a failure probability.

64 This paper proposes a practical framework for uncertainty analysis using
65 dependent p-boxes in which copulas describe the dependence. The Akaike
66 Information Criterion is used to select the copula model that provides the
67 best fit to the observational data. The confidence intervals of the copula pa-
68 rameter are estimated using the Bootstrap method. The dependent p-boxes
69 are propagated through interval Monte Carlo (MC) simulation in order to
70 assess structural reliability. The framework is applied to the time-dependent
71 reliability analysis of steel structures subject to atmospheric correlations, and
72 is demonstrated through two examples. The importance of epistemic uncer-
73 tainty in the probabilistic modeling including dependencies is demonstrated
74 on its influence on the reliability estimates.

75 **2. Dependent Probability boxes**

76 *2.1. Probability boxes with dependencies*

77 Let $F_X(x)$ denote the cumulative distribution function (CDF) for a real-
78 valued random variable X . A probability box is defined by a pair of CDFs,

79 $\underline{F}_X(x)$ and $\overline{F}_X(x)$, which form the envelopes of the probability family

$$\mathcal{P} = \{P | \forall x \in \mathbb{R}, \underline{F}_X(x) \leq F_X(x) \leq \overline{F}_X(x)\}. \quad (1)$$

80 A p-box thus represents an $F_X(\cdot)$ which is imprecisely known except that it
81 is within the two bounding CDFs. It can be seen that $\underline{F}_X(\cdot)$ and $\overline{F}_X(\cdot)$ are
82 the lower and upper probabilities of the event $X \leq x$. Detailed background
83 can be found elsewhere [7]. There are various ways to define p-boxes such as
84 utilizing Kolmogorov-Smirnov (K-S) confidence limits, Chebyshev's inequality,
85 or by distributions with interval parameters, depending on the amount of
86 available information [14].

87 The modeling of dependencies between probability boxes follows the con-
88 cept of dependence between random variables. Both Pearson correlation and
89 rank correlation have been adopted for p-boxes, but retaining their limita-
90 tions known from probability theory. Thus, copula models have been sug-
91 gested to describe dependence between p-boxes [15]. There are two main
92 advantages of using copulas for this purpose. First, copulas can account for
93 various types of dependencies. Second, the copula is flexible in selecting the
94 appropriate dependence model independently from choosing the marginal
95 distributions for each variable [16].

96 2.2. A brief introduction of copulas

97 A copula is a multivariate CDF for which the marginal distribution of
98 each variable is uniform. According to Sklar's Theorem, a joint distribution
99 can be expressed in terms of the marginal distribution functions and a copula
100 which describes the dependence structure between the variables. Consider
101 a d -dimensional random vector $\mathbf{X} = (X_1, X_2, \dots, X_d)$ with margins $F_i(x)$,
102 $i = 1, \dots, d$. There exists a copula C such that the joint CDF, denoted by

103 $F_{\mathbf{X}}(x_1, \dots, x_d)$, can be written as

$$F_{\mathbf{X}}(x_1, \dots, x_d) = C(F_1(x_1), \dots, F_d(x_d)). \quad (2)$$

104 There are two common classes of copulas; Gaussian and Archimedean.
 105 The Gaussian copula is used for the normal dependence structure. This
 106 structure can be estimated from its only parameter of a correlation matrix
 107 [17]. In a non-normal case, Archimedean copulas are often used to model the
 108 dependence structure in the data. The class of copula has a closed-form of
 109 representation,

$$C(u_1, u_2, \dots, u_d, \theta) = \varphi^{-1}(\varphi(u_1), \varphi(u_2), \dots, \varphi(u_d, \theta)), \quad (3)$$

110 in which φ is a generator with φ^{-1} completely monotonic on $[0, \infty) \times [0, \infty) \dots \times$
 111 $[0, \infty)$ (d-dimensional copula). The copula parameter, θ , can be related to
 112 various dependence structures of Archimedean copulas. The most common
 113 Archimedean copulas include Clayton, Gumbel and Frank copulas which are
 114 summarised in Table 1. Details about copulas can be found elsewhere, e.g.,
 115 [18].

Table 1: Some common Archimedean copulas.

Copula	Form	Range of θ
Clayton	$C(u_1, u_2, \theta) = (u_1^{-\theta} + u_2^{-\theta} - 1)^{-1/\theta}$	$(0, \infty)$
Frank	$C(u_1, u_2, \theta) = -\theta^{-1} \log \left\{ 1 + \frac{(e^{-\theta u_1} - 1)(e^{-\theta u_2} - 1)}{e^{-\theta} - 1} \right\}$	\mathbb{R}
Gumbel	$C(u_1, u_2, \theta) = \exp \left(- \left((-\log(u_1))^\theta + (-\log(u_2))^\theta \right)^{1/\theta} \right)$	$[1, \infty)$

116 *2.3. Estimation of copula parameter*

117 Different copulas represent different dependence structures on the data.
118 Thus, we establish the copula model in two steps. Step 1 is devoted to
119 estimate the parameters for a number of candidate copulas. The copulas
120 considered in this paper (e.g., Clayton, Gumbel and Frank copulas) involve
121 only one parameter, denoted by θ . The copula parameter θ can be estimated
122 by the classical maximum likelihood estimation (MLE). The MLE yields a
123 point **estimate** of θ .

124 In step 2 the best-fit copula model for the given observed data and (point-)
125 estimated parameter is selected. This is realized based on the Akaike Infor-
126 mation Criterion (AIC), which has particular suitability for best fit estima-
127 tions when the samples are small [19]. The AIC is given by

$$\text{AIC} = -2 \log L + 2q, \quad (4)$$

128 in which $\log L$ is the log-likelihood function and q is the number of parameters
129 of the copula model [20]. A copula model with a smaller AIC-value fits the
130 data better.

131 When the observational data is quite limited, it is desirable to calculate
132 an interval estimate of θ to indicate the range over which the copula may lie
133 with a certain confidence. The present work uses the Bootstrap method [21]
134 to construct confidence intervals of copula parameters.

135 Suppose we have n pairs of data points $(\{x_1, y_1\}, \dots, \{x_n, y_n\})$ represent-
136 ing two dependent random variables X and Y . We aim to estimate the
137 copula $C(X, Y)$ to characterize their dependence. The procedure of comput-
138 ing the $100(1 - 2\alpha)\%$ confidence interval for the copula parameter θ can be
139 summarized as follows

- 140 1. Compute a point estimate, $\hat{\theta}$, for θ from the original dataset.

- 141 2. Construct a Bootstrap sample $(\{x_1^*, y_1^*\}, \dots, \{x_n^*, y_n^*\})$. Compute the
142 copula parameter θ^* and the Bootstrap difference $\delta^* = \theta^* - \hat{\theta}$.
- 143 3. Repeat Step 2 for B times. Thus, we obtain $(\delta_1^*, \dots, \delta_B^*)$, in which δ_i^*
144 represents the Bootstrap difference for the i th Bootstrap sample.
- 145 4. Determine the $100(\alpha)$ th and $100(1 - \alpha)$ th percentile of $(\delta_1^*, \dots, \delta_B^*)$,
146 denoted by δ_α^* and $\delta_{1-\alpha}^*$. Then $100(1 - 2\alpha)\%$ confidence interval for θ
147 is calculated as $[\hat{\theta} - \delta_\alpha^*, \hat{\theta} - \delta_{1-\alpha}^*]$.

148 3. Interval Monte Carlo simulation with dependent p-boxes

149 We follow the concept of propagating p-boxes using simulation-based
150 methods (e.g., interval Monte Carlo simulation or similar approaches) [22–
151 25]. Consider a mapping $g : \mathbf{X} \rightarrow Y$, $\mathbf{X} = (X_1, X_2)$ are basic variables
152 represented by p-boxes. Further, X_1 and X_2 are dependent through a copula
153 C . The response quantity Y , as a function of X_1 and X_2 , is another p-box.
154 Let $F_Y(y)$ denote the CDF of Y . We are interested to determine the p-box
155 structure for the response quantity Y , i.e., bounds on $F_Y(y)$.

156 Monte Carlo simulation involves repeated random sampling from each
157 input distribution and to observe the result. Since only the bounds of CDF's
158 for \mathbf{X} are known, it is not possible to generate point samples but only interval
159 samples. Let $[\overline{F}_{X_1}, \underline{F}_{X_1}]$ and $[\overline{F}_{X_2}, \underline{F}_{X_2}]$ be upper and lower bounds of CDF
160 for X_1 and X_2 . Random interval samples from X_1 and X_2 can be generated
161 as follows.

- 162 1. Generate a sample of N dependent uniform variate $(\{u_1^i, u_2^i\}, i = 1, \dots, N)$
163 from the specified copula C .

2. Generate pairs of dependent random interval samples by

$$\begin{aligned} [\underline{x}_1^i, \bar{x}_1^i] &= [\underline{F}_{X_1}^{-1}(u_1^i), \bar{F}_{X_1}^{-1}(u_1^i)], \\ [\underline{x}_2^i, \bar{x}_2^i] &= [\underline{F}_{X_2}^{-1}(u_2^i), \bar{F}_{X_2}^{-1}(u_2^i)], \quad i = 1, 2, \dots, N \end{aligned}$$

164 in which \bar{F}^{-1} and \underline{F}^{-1} denotes the inverse functions of upper and lower
165 bounds of a p-box.

166 For the sampling in the first step we utilize a **common** method, see e.g.,
167 [18]:

- 168 1. Generate two independent standard uniform variates u_1 and t .
- 169 2. Set $u_2 = c_u^{-1}(t)$, where c_u^{-1} denotes a quasi-inverse of c_u .
- 170 3. $\{u_1, u_2\}$ is a pair of uniform variates with the specified copula C .

Once the correlated random interval samples are generated, the empirical lower and upper bounds for the CDF of Y can be calculated as

$$\begin{aligned} \underline{F}_Y(y) &= \frac{1}{N} \sum_{i=1}^N \mathbf{I}[\underline{g}(\mathbf{x}_i) \leq y], \\ \bar{F}_Y(y) &= \frac{1}{N} \sum_{i=1}^N \mathbf{I}[\bar{g}(\mathbf{x}_i) \leq y], \end{aligned} \quad (5)$$

in which $N =$ total number of simulations, $\mathbf{x}_i = ([\underline{x}_1^i, \bar{x}_1^i], [\underline{x}_2^i, \bar{x}_2^i])$, $\mathbf{I}[\]$ is the indicator function, having the value 1 if $[\]$ is “true” and the value 0 if $[\]$ is “false”. \underline{g} and \bar{g} represent a lower bound and an upper bound for $g(\mathbf{x}_i)$, i.e.,

$$\begin{aligned} \underline{g}(\mathbf{x}_i) &= \min\{g(X_1, X_2) : \underline{x}_1^i \leq X_1 \leq \bar{x}_1^i, \underline{x}_2^i \leq X_2 \leq \bar{x}_2^i\}, \\ \bar{g}(\mathbf{x}_i) &= \max\{g(X_1, X_2) : \underline{x}_1^i \leq X_1 \leq \bar{x}_1^i, \underline{x}_2^i \leq X_2 \leq \bar{x}_2^i\}. \end{aligned} \quad (6)$$

171 Computing Eq. (6) involves the calculation of the range of function g
172 when the inputs vary in certain closed intervals. The problem of finding
173 the range of a function is solved on the basis of interval analysis [26]. A

174 variety of solution techniques have been proposed, including the interval
175 arithmetic approach, combinatorial method, perturbation method, and opti-
176 mization method, etc. Reliable methods are available to compute the bounds
177 of responses of structures with reasonable accuracy when the structural stiff-
178 ness and geometrical properties and loads vary in relatively narrow intervals
179 [27]. It should be noted that the burden of interval analysis can be reduced
180 if the response quantity Y is monotonic with respect to the input variables.

181 **4. Atmospheric corrosion model for steel structures**

182 For steel structures, corrosion is considered as the most dominant form of
183 deterioration. Corrosion is a product of the chemical reaction by electrochem-
184 ical oxidation of metals and oxidant when a steel surface is left unprotected
185 from the environment. This chemical reaction causes a reduction in net area
186 of a member; thus, it leads to a reduction in the structural capacity of a steel
187 member.

188 Depending on the environment where the steel is exposed, corrosion pro-
189 cesses can be broadly classified as atmospheric corrosion, immersion corrosion
190 and underground corrosion. The present paper considers the atmospheric
191 corrosion in rural-urban environment to illustrate the proposed uncertainty
192 analysis framework. It should be noted that corrosions due to salted air
193 (marine atmospheric corrosion), de-icing chemical, etc. have higher impact
194 to the failure of a structure. However, they are beyond the scope of the
195 present study.

196 The available models for time-variant atmospheric corrosion of steel are
197 commonly based on the mass loss or penetration depth loss from experiments.
198 They include time variable and several regression coefficients in the form of
199 power formula to capture the corrosion process. A widely-accepted model

200 for long-term atmospheric corrosion of steel conforms to an equation of the
201 form [28–30]:

$$c(t) = A \cdot t^B, \quad (7)$$

202 in which $c(t)$ is the corrosion loss after t years, A is the corrosion loss af-
203 ter one year, and B is a constant representing the slope of the logarithmic
204 transformation of Eq. (7). The power function was derived based on the
205 diffusional process of oxygen through rust layers. Due to its simplicity, the
206 power function has a long history in modelling of atmospheric corrosion for
207 steel structures [31, 32]. This model was adopted in the present study.

208 4.1. *Uncertainties in the corrosion model*

209 The coefficients A and B in Eq. (7) were studied in [29, 33]. The study
210 showed that A and B are dependent on environmental parameters including
211 ambient temperature, moisture of environment and presence of pollutants,
212 etc. If the site-specific environment information is not available, the val-
213 ues of A and B can be estimated according to the general classification of
214 environment, i.e., marine, urban and rural environment.

215 The present study focuses on the modelling of atmospheric corrosion of
216 carbon steels exposed in rural-urban environments. A total of 62 atmospheric
217 corrosion data in rural-urban environment are compiled from the literature
218 [34–38]. These corrosion data are fitted with Eq. (7) and the coefficients A
219 and B are determined. The obtained statistics (point estimates) of A and B
220 are summarised in Table 2.

221 It can be seen that the results from these studies are quite consistent.
222 Most studies show that A has a mean of about 30 μm with a high COV
223 (coefficient of variation) around 0.3, and the coefficient B has a mean around
224 0.55 with a COV varying between 0.1 to 0.3. (Note that there are only two

225 samples in [37]. The data can be used to estimate the mean values, but is
 226 insufficient to estimate the variance.) If the data from the five sources are
 227 lumped together, A has a mean of 29.1 μm and a COV of 0.31, and B has
 228 a mean of 0.54 with a COV of 0.21. Many researchers assumed that A and
 229 B follow normal distributions, e.g., [39]. This assumption is adopted in the
 230 present study.

231 Four types of copula were examined to represent the dependence between
 232 A and B : Frank, Clayton, Gumbel and Gaussian copulas. The copula pa-
 233 rameters were estimated using the maximum likelihood method. Among the
 234 four candidate copulas, the Frank copula with a parameter $\theta = -1.85$ yields
 235 the smallest value of AIC, thus it provides the best-fit to the dependence
 236 structure of A and B .

Table 2: Statistics for corrosion coefficients A and B (rural-urban environment).

References	A		B		No. samples
	Mean (μm)	COV	Mean	COV	
[34]	24.5	0.22	0.501	0.23	12
[35]	28.36	0.29	0.571	0.19	14
[36]	30.74	0.32	0.583	0.07	19
[37]	23.5	—	0.516	—	2
[38]	32	0.31	0.502	0.30	15
Combined	29.1	0.31	0.54	0.21	62

237 In addition to the randomness in A and B , we next consider the addi-
 238 tional uncertainty (epistemic uncertainty) arising from the inaccuracies in the
 239 estimation of distribution parameters due to limited data, namely, the mean
 240 values of A and B (denoted by μ_A and μ_B), and the copula parameter θ . The
 241 imperfect knowledge about μ_A , μ_B and θ can be modelled by interval bounds

242 constructed from confidence intervals. The 95% confidence intervals for μ_A
 243 and μ_B are $\mu_A = [26.83, 31.37]$ and $\mu_B = [0.51, 0.57]$. Using the Bootstrap
 244 method, the 95% confidence interval for θ is found to be $\theta = [-3.35, -0.35]$.

245 Depending on the modeling of the distribution parameters, the present
 246 study considers 6 cases, as summarised in Table 3. Case 1 uses the point
 247 estimates for μ_A , μ_B and θ . This case represents the customary practice in
 248 which the epistemic uncertainties due to small sample size are not consid-
 249 ered. Case 2 considers the interval estimate of θ , while μ_A and μ_B are point
 250 estimates. In Case 3, both μ_A and μ_B are modeled as intervals, while θ is a
 251 point estimate. To examine the sensitivities of each of the parameters (μ_A ,
 252 μ_B and θ) on the failure probability P_f , Case 3 is further divided into Case
 253 3a and Case 3b. In Case 3a, μ_A is an interval estimate, while μ_B and θ are
 254 point estimates. In Case 3b, μ_B is an interval estimate, while μ_A and θ are
 255 point estimates. Thus, by comparing Case 2, 3a and 3b, the impacts of μ_A ,
 256 μ_B and θ on P_f can be quantified, respectively. In Case 4, all parameters,
 257 μ_A , μ_B and θ , are modeled as intervals.

Table 3: Six cases for modeling A (unit: μm) and B .

	A		B		copula parameter
	μ_A	σ_A	μ_B	σ_B	
Case 1	29.1	9.13	0.54	0.11	$\theta = -1.85$
Case 2	29.1	9.13	0.54	0.11	$\theta = [-3.35, -0.35]$
Case 3	[26.83, 31.37]	9.13	[0.51, 0.57]	0.11	$\theta = -1.85$
Case 3a	[26.83, 31.37]	9.13	0.54	0.11	$\theta = -1.85$
Case 3b	29.1	9.13	[0.51, 0.57]	0.11	$\theta = -1.85$
Case 4	[26.83, 31.37]	9.13	[0.51, 0.57]	0.11	$\theta = [-3.35, -0.35]$

258 5. Examples

259 5.1. Example 1: a steel plate

260 A steel plate in tension is studied. The problem is adopted from [40].
261 The limit state function is given by:

$$g = R(t) - S, \quad (8)$$

262 in which S is the applied tensile load, and $R(t)$ is the time-variant resistance
263 of the plate. Let b and d denote the nominal width and thickness of the
264 plate, respectively. The plate is assumed to be corroded in the rural-urban
265 environment on two sides, thus the temporal change to the plate thickness
266 is $d - 2c(t)$, in which $c(t)$ represents the corrosion loss after t years. The
267 time-dependent structural resistance is given by:

$$R(t) = f_y b (d - 2c(t)), \quad (9)$$

268 in which f_y is the yield stress. The applied load S is assumed to be a normal
269 distribution with a mean of 200 kN and a standard deviation of 23 kN. The
270 yield stress f_y is a normal random variable with a mean of 300 MPa and a
271 standard deviation of 10 MPa. The width b and the original thickness d are
272 deterministic, and $b = 250$ mm, $d = 4$ mm. The corrosion loss c is computed
273 according to Eq. (7).

274 To verify the reliability results from the interval Monte Carlo method, a
275 double-loop Monte Carlo procedure is utilized to compute the bounds of P_f
276 for Case 2 and Case 3 at $t = 20$ year and $t = 50$ year. In the double-loop
277 Monte Carlo procedure, the interval parameter(s) is assumed to uniformly
278 distribute between its lower and upper bounds. Two hundred samples of the
279 interval parameter was generated in the outer loop using the Latin Hyper-
280 cube sampling technique. With each sampled parametric value, the failure

281 probability was then evaluated in the inner loop. Thus a sample of P_f can
 282 be obtained; its lower and upper bounds are then compared with the P_f
 283 bounds computed using the interval Monte Carlo method. Tables 4 and 5
 284 compare the bounds of P_f in $t = 20$ year and $t = 50$ year obtained from
 285 the double-loop Monte Carlo and the interval Monte Carlo methods. It can
 286 be seen that the results from the two methods agree reasonably well. The
 287 bounds of P_f from the interval Monte Carlo method are slightly wider than
 288 those of the double-loop Monte Carlo method.

Table 4: Comparison of double-loop Monte Carlo and interval Monte Carlo methods: P_f in $t = 20$ yr, (Example 1).

	Case 2		Case 3	
	$\underline{P}_f(\%)$	$\overline{P}_f(\%)$	$\underline{P}_f(\%)$	$\overline{P}_f(\%)$
Interval MC	0.049	0.727	0.116	0.410
Double-loop MC	0.051	0.682	0.121	0.387

Table 5: Comparison of double-loop Monte Carlo and interval Monte Carlo methods: P_f in $t = 50$ yr, (Example 1).

	Case 2		Case 3	
	$\underline{P}_f(\%)$	$\overline{P}_f(\%)$	$\underline{P}_f(\%)$	$\overline{P}_f(\%)$
Interval MC	0.297	10.082	1.394	5.719
Double-loop MC	0.307	9.245	1.455	5.356

289 The all six cases in Table 3 are then considered. The failure probability
 290 P_f for the six cases are plotted in Figs. 1 and 2 as a function of time. The
 291 results for $t = 20$ yr and 50 yr are also summarised in Table 6.

292 In Table 6, P_f is a point estimate for Case 1; it is 0.208% for $t = 20$
 293 year and 2.910% for $t = 50$ year. This point estimate of P_f does not provide

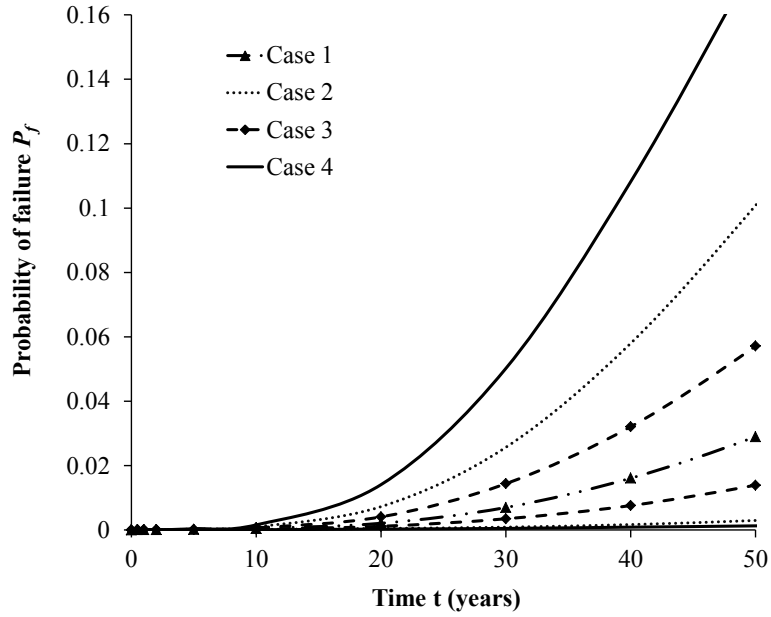


Figure 1: Bounds of the failure probabilities of Example 1 (Case 1-4).

Table 6: Probability of failure (Example 1).

	$t = 20$ years		$t = 50$ years	
	\underline{P}_f	\overline{P}_f	\underline{P}_f	\overline{P}_f
Case 1		0.208%		2.910%
Case 2	0.049%	0.727%	0.297%	10.082%
Case 3	0.116%	0.410%	1.394%	5.719%
Case 3a	0.166%	0.283%	2.212%	3.733%
Case 3b	0.149%	0.308%	1.847%	4.449%
Case 4	0.029%	1.382%	0.131%	17.650%

294 information about the confidence in the result of the reliability estimate. The
 295 role of epistemic uncertainty on P_f is clearly demonstrated in the bounds of
 296 P_f shown in Figure 1 and Table 6. The width of the interval P_f shows the
 297 effect of epistemic uncertainty on the results of the reliability estimate. For

298 example, the upper bound of P_f for $t = 50$ year is 10.082% for Case 2. This
299 probability is an order of magnitude greater than the point estimate from
300 Case 1. A point estimate without considering the epistemic uncertainty may
301 significantly underestimate the true risk.

302 It can be seen from Figure 1 that the interval bounds of P_f become wider
303 as time increases. Take Case 3 for example, P_f varies from [0.116%, 0.410%]
304 at $t = 20$ yr, and increases significantly to [1.394%, 5.719%] at $t = 50$ yr. It
305 is also observed that the width of P_f for Case 2 is much wider than that of
306 Case 3. For instance, at $t = 50$ year, P_f is [0.297%, 10.082%] for Case 2, and
307 [1.394%, 5.719%] for Case 3. The width of the former is more than twice of the
308 latter. This suggests that the epistemic uncertainty in the copula modeling
309 the dependence between A and B has a more significant effect on P_f than
310 the epistemic uncertainty in the mean values of A and B . As expected, the
311 width of P_f becomes wider when the analysis incorporates more epistemic
312 uncertainties, i.e., the interval failure probabilities for Case 2 and Case 3 are
313 enclosed in the P_f for Case 4.

314 To study the sensitivity of the parameters, μ_A , μ_B and θ , on the failure
315 probability, we compare the results of Case 2, Case 3a and Case 3b. The time-
316 dependent probabilities of failure for the three cases are plotted in Figure 2.
317 The results for $t = 20$ yr and $t = 50$ yr are also presented in Table 6. It is
318 observed from Figure 2 that the width of P_f for Case 2 is much wider than
319 those of Case 3a and Case 3b. This suggests that the uncertainty in the
320 dependence between A and B has a more significant effect on P_f than the
321 epistemic uncertainties in μ_A and μ_B . Table 6 and Fig. 2 also shows that
322 the widths of P_f for Case 3a and Case 3b are comparable, implying that the
323 uncertainties in μ_A and μ_B have similar effects on P_f . This sensitivity study
324 shows that to improve the confidence in the reliability estimates, additional

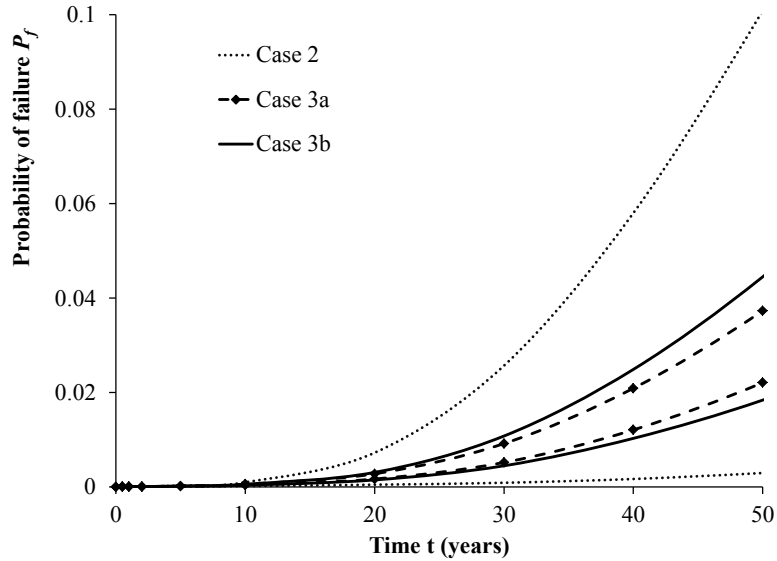


Figure 2: Bounds of the failure probabilities of Example 1 (Case 2, Case 3a and Case 3b).

325 data should be collected, particularly for modeling the dependence between
 326 A and B .

327 5.2. Example 2: a ten-bar truss

328 Figure 3 shows a ten-bar planar steel truss subjected to two concentrated
 329 loads P . The example is adopted from [41]. The truss members are circular
 330 hollow section (CHS) with three different sections, A_1 , A_2 and A_3 , for the
 331 horizontal, vertical and diagonal members, respectively. The nominal section
 332 sizes (outer diameter) and thickness are summarised in Table 7. The basic
 333 random variables include the load P , the thickness of CHS r_i , $i = 1, 2, 3$,
 334 and the Young's modulus E . These random variables are assumed to be
 335 mutually statistically independent normal distributions, with the statistics
 336 summarised in Table 8. The outer diameters of the sections are assumed to
 337 be deterministic and equal to their nominal values.

338 The limit state of interest is the stress in the diagonal member 1. The

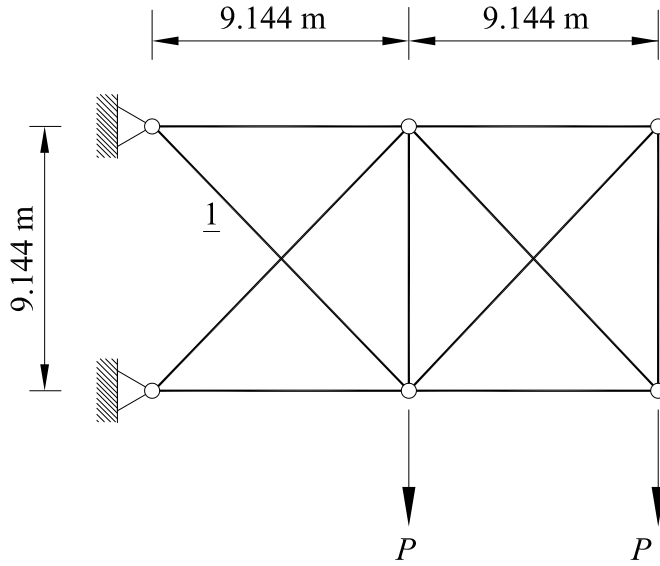


Figure 3: A ten-bar steel truss (adopted from [41]).

Table 7: Nominal section sizes for the ten-bar truss.

Section	d (outer diameter)	r (thickness)
A_1	243.8 mm	8.8 mm
A_2	193 mm	2.9 mm
A_3	243.8 mm	7.4 mm

Table 8: Random variables for the ten-bar truss.

Variable	Unit	Mean	COV (%)	Distribution
P	kN	444.8	20	Normal
r_1	mm	8.8	8	Normal
r_2	mm	2.9	8	Normal
r_3	mm	7.4	8	Normal
E	GPa	205	6	Normal

339 stress, σ_1 , is given by a closed-form solution [41]:

$$\sigma_1 = \frac{P}{A_3} \left(2 + \frac{\sqrt{2}A_1A_2A_3(2\sqrt{2}A_1 + A_3)}{D} \right), \quad (10)$$

where

$$D = 4A_2^2(8A_1^2 + A_3^2) + 4\sqrt{2}A_1A_2A_3(3A_1 + 4A_2) + A_1A_3^2(A_1 + 6A_2). \quad (11)$$

340 The limit state function, $g(\cdot)$, is defined as

$$g = \sigma_a - \sigma_1 \quad (12)$$

341 in which the allowable stress σ_a is 250 MPa.

342 Considering the atmospheric deterioration of the steel and assuming two-
343 sided corrosion loss, the cross-section areas $A_i(t)$ change with time t :

$$A_i(t) = \left(\frac{d_i^2\pi}{4} - \frac{(d_i - 2r_i)^2\pi}{4} \right) - \left(\frac{d_i^2\pi}{4} - \frac{(d_i - 2c(t))^2\pi}{4} \right), \quad i = 1, 2, 3. \quad (13)$$

344 in which d_i and r_i denote the outer diameter and thickness for the CHS
345 members, and $c(t)$ is the corrosion loss after t years.

346 Cases 2, 3a and 3b are first studied to examine the sensitivity of each
347 parameter, μ_A , μ_B and θ , on the failure probability. The lower and upper
348 bounds of the failure probabilities for the three cases are plotted in Fig. 4.
349 Next, all six cases listed in Table 3 are studied. Figure 5 plots the lower
350 and upper bounds of P_f as a function of time for Case 1-4. Table 9 presents
351 the probability of failure for $t = 30$ year and $t = 50$ year. From Figs. 4 and
352 5, and Table 9, similar observations can be made as in Example 1. Case 4
353 has the widest bounds, followed by Case 2, 3 and 1. The results confirm
354 that 1) the epistemic uncertainty has a significant impact on the reliability
355 estimates, 2) the epistemic uncertainty in the copula parameter θ has a far

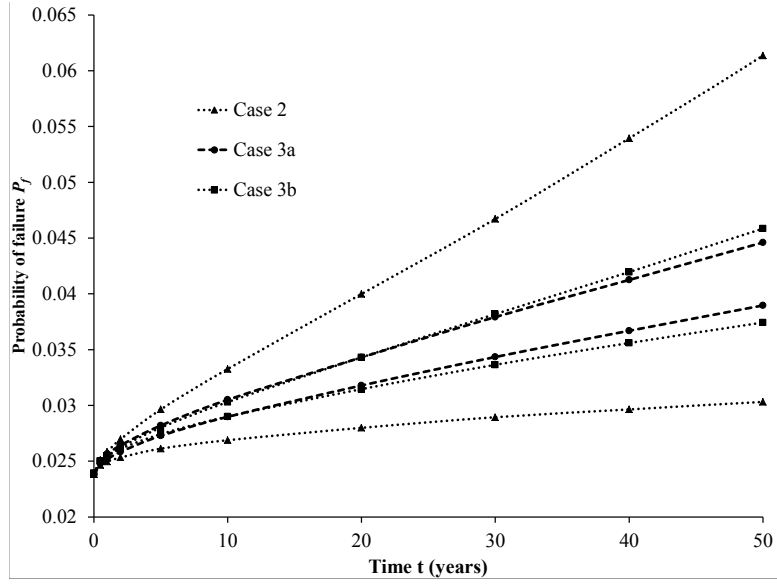


Figure 4: Bounds of the failure probabilities of Example 2 (Case 2, Case 3a and Case 3b).

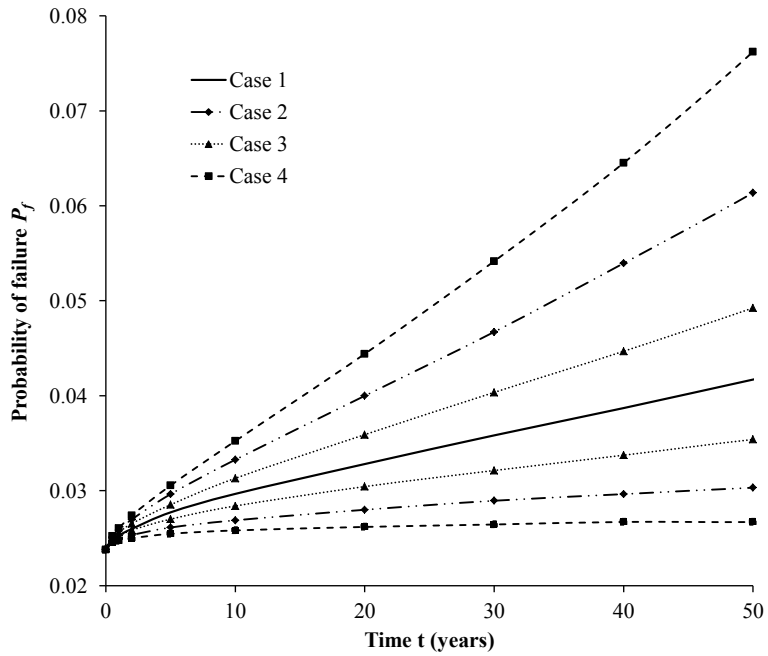


Figure 5: Bounds of the failure probabilities of Example 2 (Case 1-4).

Table 9: Probability of failure of member 1 of the 10-bar truss.

	$t = 30$ yr		$t = 50$ yr	
	\underline{P}_f	\overline{P}_f	\underline{P}_f	\overline{P}_f
Case 1	0.0359		0.0414	
Case 2	0.0288	0.0466	0.0302	0.0612
Case 3	0.0321	0.0402	0.0352	0.0491
Case 3a	0.0343	0.0378	0.0389	0.0445
Case 3b	0.0336	0.0382	0.0374	0.0456
Case 4	0.0265	0.0541	0.0268	0.0764

356 more significant effect on P_f than the epistemic uncertainties in the means
 357 of A and B , and 3) the epistemic uncertainties in the mean values of A of B
 358 have comparable effects on P_f .

359 6. Conclusions

360 Significant epistemic uncertainties exist in the current models for atmo-
 361 spheric corrosion of steel structures due to the limited availability of reliable
 362 corrosion data. Probability-box is a useful tool to model the uncertain cor-
 363 rosion process, accounting for both the aleatory and epistemic uncertainties.
 364 **In the present study, the epistemic uncertainties are vested in the estimates**
 365 **of the first-order statistics (mean) of the corrosion coefficients A and B , and**
 366 **also the dependence structure between A and B .** By examining available
 367 corrosion data, it is found that the dependence between A and B can be
 368 modeled by a Frank copula. The confidence intervals of the copula parame-
 369 ter are estimated using the Bootstrap method. Interval Monte Carlo method
 370 are used to compute the lower and upper bounds of probability of failure.

371 The probability-box analysis framework was applied to the time-dependent

372 reliability analysis of a steel plate and a steel truss structures. In both ex-
373 amples, similar observations are made. The epistemic uncertainties play an
374 important role in the reliability assessment. A point estimate of P_f without
375 considering any epistemic uncertainty may lead to a false impression of the
376 reliability. The interval bounds of P_f become wider as time increases. **It**
377 **was also found that the epistemic uncertainty in the dependence between A**
378 **and B (vested in the copula parameter θ) has a far more significant effect**
379 **on P_f than the epistemic uncertainty in the means of A and B . The epis-**
380 **temic uncertainties in the mean values of A and B have comparable effects**
381 **on P_f .** The importance of collecting more corrosion data, particularly for
382 modeling the dependence of A and B , is demonstrated if the confidence in
383 the reliability assessment is to be improved.

384 **Acknowledgments**

385 Support for this research was provided, in part, by the Lawrence and
386 Betty Brown PhD Research Scholarship in Civil Engineering, the Civil En-
387 gineering Research Development Scheme from the University of Sydney, and
388 the International Program Development Fund from the University of Syd-
389 ney. These supports are gratefully acknowledged. **The authors would like to**
390 **acknowledge the thoughtful suggestions of two anonymous reviewers, which**
391 **substantially improved the present paper.**

392 **References**

- 393 [1] Q. Li, C. Wang, B. Ellingwood, Time-dependent reliability of aging
394 structures in the presence of non-stationary loads and degradation,
395 Struct. Saf. 52A (2015) 132–141.

- 396 [2] H. Dai, B. Zhang, W. Wang, A multiwavelet support vector regression
397 method for efficient reliability assessment, *Reliab. Engng. Syst. Saf.* 136
398 (2015) 132–139.
- 399 [3] Q. Li, C. Wang, Updating the assessment of resistance and reliability of
400 existing aging bridges with prior service loads, *J. Struct. Engrg., ASCE*
401 141 (12) (2015) 04015072.
- 402 [4] H. Dai, H. Zhang, W. Wang, A multiwavelet neural network-based re-
403 sponse surface method for structural reliability analysis, *Compu.-Aided*
404 *Civ. Infrastruct. Engrg.* 30 (2) (2015) 151–162.
- 405 [5] B. R. Ellingwood, K. Kinali, Quantifying and communicating uncer-
406 tainty in seismic risk assessment, *Struct. Saf.* 31 (2009) 179–187.
- 407 [6] P. Walley, *Statistical reasoning with imprecise probabilities*, Chapman
408 and Hall, London, 1991.
- 409 [7] S. Ferson, V. Kreinovich, L. Ginzburg, D. S. Myers, K. Sentz, Con-
410 structing probability boxes and Dempster-Shafer structures, *Tech. Rep.*
411 *SAND2002-4015*, Sandia National Laboratories (2003).
- 412 [8] P. Walley, Towards a unified theory of imprecise probability, *Int. J.*
413 *Approximate Reasoning* 24 (2000) 125–148.
- 414 [9] B. Möller, M. Beer, Engineering computation under uncertainty-
415 capabilities of non-traditional models, *Comput. Struct.* 86 (10) (2008)
416 1024–1041.
- 417 [10] C. Baudrit, D. Dubois, N. Perrot, Representing parametric probabilistic
418 models tainted with imprecision, *Fuzzy Sets Syst.* 159 (2008) 1913–1928.

- 419 [11] P. Walley, T. Fine, Towards a frequentist theory of upper and lower
420 probability, *Ann. Stat.* 10 (1982) 741–761.
- 421 [12] S. Ferson, R. B. Nelsen, J. Hajagos, D. J. Berleant, J. Zhang, W. T.
422 Tucker, L. R. Ginzburg, W. L. Oberkampf, Dependence in probabilistic
423 modeling, Dempster-Shafer theory, and probability bounds analysis, Re-
424 port SAND2004-3072, Sandia National Laboratories, Albuquerque, NM
425 (2004).
- 426 [13] D. A. Alvarez, J. E. Hurtado, An efficient method for the estimation of
427 structural reliability intervals with random sets, dependence modeling
428 and uncertain inputs, *Comp. Struc.* 142 (2014) 54–63.
- 429 [14] M. Zhang, M. Beer, S. Quek, Y. Choo, Comparison of uncertainty mod-
430 els in reliability analysis of offshore structures under marine corrosion,
431 *Struct. Saf.* 32 (6) (2010) 425–432.
- 432 [15] G. Salvadori, C. De Michele, Frequency analysis via copulas: Theoret-
433 ical aspects and applications to hydrological events, *Water Resources*
434 *Research* 40 (12).
- 435 [16] C. Genest, A. C. Favre, Everything you always wanted to know about
436 copula modeling but were afraid to ask, *Journal of Hydrologic Engineer-*
437 *ing* 12 (4) (2007) 347–368.
- 438 [17] B. Renard, M. Lang, Use of a gaussian copula for multivariate extreme
439 value analysis: some case studies in hydrology, *Advances in Water Re-*
440 *sources* 30 (4) (2007) 897–912.
- 441 [18] R. B. Nelsen, *An introduction to copulas*, Springer, 1999.

- 442 [19] R. H. Shumway, D. S. Stoffer, D. S. Stoffer, Time series analysis and its
443 applications, Springer, 2011.
- 444 [20] U. Cherubini, E. Luciano, W. Vecchiato, Copula methods in finance,
445 John Wiley & Sons, 2004.
- 446 [21] B. Efron, Computers and the theory of statistics: thinking the unthink-
447 able, SIAM Review 21 (4) (1979) 460–480.
- 448 [22] D. A. Alvarez, On the calculation of the bounds of probability of events
449 using infinite random sets, Int. J. Approximate Reasoning 43 (2006)
450 241–267.
- 451 [23] H. Zhang, R. L. Mullen, R. L. Muhanna, Interval Monte Carlo methods
452 for structural reliability, Struct. Saf. 32 (2010) 183–190.
- 453 [24] H. Zhang, H. Dai, M. Beer, W. Wang, Structural reliability analysis
454 on the basis of small samples: an interval Monte Carlo method, Mech.
455 Systems Signal Process. 37 (2013) 137–151.
- 456 [25] H. Zhang, Interval importance sampling method for finite element-based
457 structural reliability assessment under parameter uncertainties, Struct.
458 Saf. 38 (2012) 1–10.
- 459 [26] R. E. Moore, Interval Analysis, Prentice-Hall, Inc., Englewood Cliffs,
460 N. J., 1966.
- 461 [27] H. Zhang, Nondeterministic linear static finite element analysis: an in-
462 terval approach, Ph.D. thesis, Georgia Institute of Technology, Atlanta,
463 GA, USA (2005).

- 464 [28] D. De la Fuente, I. Daz, J. Simancas, B. Chico, M. Morcillo, Long-term
465 atmospheric corrosion of mild steel, *Corrosion Science* 53 (2) (2011)
466 604–617.
- 467 [29] S. Feliu, M. Morcillo, S. Feliu Jr, The prediction of atmospheric corrosion
468 from meteorological and pollution parameters–II. long-term forecasts,
469 *Corrosion Science* 34 (3) (1993) 415–422.
- 470 [30] R. H. McCuen, P. Albrecht, Composite modeling of atmospheric corro-
471 sion penetration data, *ASTM Special Technical Publication* 1194 (1994)
472 65–65.
- 473 [31] M. Morcillo, B. Chico, I. Daz, H. Cano, D. De la Fuente, Atmospheric
474 corrosion data of weathering steels. a review, *Corrosion Science* 77 (2013)
475 6–24.
- 476 [32] ISO-9223, Corrosion of metals and alloys–Corrosivity of atmospheres.
477 Classification, determination and estimation, International Organization
478 for Standardization (2012).
- 479 [33] S. Feliu, M. Morcillo, S. Feliu Jr, The prediction of atmospheric corro-
480 sion from meteorological and pollution parameters–I. annual corrosion,
481 *Corrosion Science* 34 (3) (1993) 403–414.
- 482 [34] F. Haynie, J. B. Upham, Effects of atmospheric pollutants on corrosion
483 behavior of steels, *Materials Protection and Performance* 10 (1971) 18–
484 21.
- 485 [35] L. Atteraaas, S. Haagenrud, Atmospheric corrosion testing in Norway,
486 John Wiley & Son, New York, USA, 1982, pp. 873–891.

- 487 [36] V. Kucera, S. Haagenrud, L. Atteraas, J. Gullman, S. Dean, T. Lee, Cor-
488 rosion of steel and zinc in scandinavia with respect to the classification of
489 the corrosivity of atmospheres, *Degradation of Metals in Atmospheres*,
490 ASTM STP 965 (1987) 264–281.
- 491 [37] H. D. Hui, P. Strekalov, Y. N. Mikhailovskii, D. T. BIN, A. Mikhailov,
492 The corrosion-resistance of steels, zinc, copper, aluminum, and alloys in
493 the humid tropics of vietnam-the results of 5-year tests, *Protection of*
494 *Metals* 30 (5) (1994) 437–443.
- 495 [38] M. Morcillo, J. Simancas, S. Feliu, Long-term atmospheric corrosion in
496 spain: results after 13 to 16 years of exposure and comparison with
497 worldwide data, *ASTM special technical publication* 1239 (1995) 195–
498 195.
- 499 [39] M. Chakravorty, D. M. Frangopol, R. L. Mosher, J. E. Pytte, Time-
500 dependent reliability of rock-anchored structures, *Reliab. Engng. Syst.*
501 *Saf.* 47 (3) (1995) 231–236.
- 502 [40] R. E. Melchers, Probabilistic model for marine corrosion of steel for
503 structural reliability assessment, *J. Struct. Engrg.*, ASCE 129 (11)
504 (2003) 1484–1493.
- 505 [41] S.-K. Choi, R. V. Grandhi, R. A. Canfield, *Reliability-based structural*
506 *design*, Springer Science & Business Media, 2006.